Maxwell

by M 3

Submission date: 04-Jul-2022 05:29PM (UTC+0800)
Submission ID: 1866510636
File name: Maxwell3.pdf (2.28M)
Word count: 7056
Character count: 33576

Collision of hybrid nanomaterials in an upper-convected Maxwell nanofluid: a theoretical approach

Hanifa Hanif[a,b,*], Sharidan Shafie[b,*], Rozaini Roslan[c,d] and Anati Ali[b]

[a]Department of Mathematics, Sardar Bahadur Khan Women's University, Quetta, Pakistan
[b]Department of Mathematical Sciences, Faculty of Science, Universiti Teknologi Malaysia, 81310 Johor Bahru, Johor, Malaysia
[c]Department of Mathematics & Statistics, Faculty of Applied Sciences and Technology, Universiti Tun Hussein Onn Malaysia, Pagoh, 84600 Muar, Malaysia
[d]ANNA Systems LLC, Moscow Region, Dubna, 9 Maya Street, Building 7B, Building 2 Office 10.141707, Moscow, Dolgoprudnenskoe Highway, 3, Fiztekhpark, Moscow 141980, Russia

ARTICLE INFO

Keywords:
Fractional calculus
Nanofluid
UCM fluid model
Viscous dissipation

ABSTRACT

Many viscoelastic fluid problems are solved using the notion of fractional derivative. However, most researchers paid little attention to the effects of nonlinear convective in fluid flow models with time-fractional derivatives and were mainly interested in solving linear problems. Furthermore, the nonlinear fluid models with a fractional derivative for an unsteady state are rare, these constraints must be overcome. On the other hand, nanofluids are thought to be trustworthy coolants for enhancing the cooling process in an electrical power system. Therefore, this research has been conducted to analyze the unsteady upper-convected Maxwell (UCM) hybrid nanofluid model with a time fractional derivative. Incorporating Cattaneo heat flux into the energy equation has increased the uniqueness of the research. The numerical solutions for the coupled partial differential equations describing velocity and temperature are presented using an efficient finite difference method assisted by Caputo fractional derivative. The graphs demonstrate the significant impact of all governing parameters on fluid flow, including the nanomaterial volume fraction, fractional derivative, relaxation time, and viscous dissipation. Furthermore, both the skin-friction coefficient and Nusselt number are discussed to illustrate the current problem more thoroughly and clearly. To manifest a surface heat increase, the nanomaterial concentration, the fractional derivative parameter, and the relaxation time parameter must all be substantial.

1. Introduction

A crucial topic in fluid dynamics is the behavior of materials with the qualities of elasticity and viscosity when they deform. The term "Maxwell fluid" has been coined to describe these kinds of

hanifahanif@outlook.com (H. Hanif); sharidan@utm.my (S. Shafie)
ORCID(s): 0000-0003-0053-0653 (H. Hanif); 0000-0001-7795-2278 (S. Shafie); 0000-0003-1526-4183 (R. Roslan)

Nomenclature

Latin Letters		$\mathcal{H}$	Heaviside function
C_p	specific heat capacity ($Jkg^{-1}K^{-1}$)	$\mathcal{T}$	Cattera-stress tensor (Nm^{-2})
k	thermal conductivity ($Wm^{-1}K^{-1}$)	μ	dynamic viscosity ($kgm^{-1}s^{-1}$)
Nu_L	Nusselt number	∇	gradient operator
p	hydrostatic pressure (Pa)	ν	kinematic viscosity (m^2s^{-1})
q	heat flux (Wm^{-2})	ρ	density (kgm^{-3})
T	temperature (K)		Cauchy stress tensor (Nm^{-2})
t	time (s)	φ	volume fraction of nanomaterials
V	velocity component in x direction (ms^{-1})	**Subscripts/Superscripts**	
Pr	Prandtl number	$*$	non-dimensional
Greek Letters		f	base fluid
α/β	fractioal derivative order	hnf	hybrid nanofluid
Δt	time step	i	grid point in x direction
Δy	grid size in y direction	j	grid point in y direction
Δz	grid size in z direction	k	time level
λ_1/λ_2	relaxation time (s)	nf	nanofluid
$\mathcal{A}_1$	Rivilin-Erickson tensor (Nm^{-2})	p_1/p_2	nanoparticles

materials, postulated by James Clerk Maxwell in 1867, and James G. Oldroyd popularized it a few years later [1, 2]. The UCM model is a function of relaxation time, stress tensor, deformation rate tensor, velocity and viscosity. It uses the Oldyrold derivative as a Maxwell material extension for massive deformations [2]. The UCM model depends on relaxation time, stress tensor, deformation rate tensor, velocity, and viscosity [3]. It uses the Oldyrold derivative as a Maxwell material extension for massive deformations [4]. The influence of thermophoretic particle deposition and magnetic dipole in the flow of Maxwell over a stretching sheet is examined by Kumar et al. [5]. The results showed that while heat and mass transmission are improved, the velocity gradient reduces by increasing the ferromagnetic interaction parameter value.

The history of fractional calculus is fairly similar to that of classical calculus. However, over the past few decades, it has grown in popularity in the structural modeling of non-Newtonian fluids. The primary reason for this advancement is that a fractional model may explain the complicated features of viscoelastic material in a simple and elegant manner. For instance, the exponential relaxation moduli of traditional ordinary models are unable to effectively describe the algebraic decay during the relaxation process of many materials [6]. Experiments, however, show that fractional models are capable of properly capturing and connecting these phenomena [7, 8]. Dalir and Bashour presented a real-world application of fractional calculus in [9]. Moreover, a comprehensive list of fractional calculus applications in science and engineering is given in [10]. Researchers demonstrated innovative use of the fractional derivative in several fluid models [11–13].

The heat transfer phenomena of nanofluid flow have recently attracted the attention of many academics because of their immense and fundamental significance from both an applied and theoretical perspective. Nanofluid is a colloidal mixture of nanometer-sized particles(metallic and

non-metallic) in a typical convectional fluid. Because of their superior thermal and tribological properties, nanofluids are considered potential heat transfer fluids. Due to this critical importance, we would like to highlight the abundance of various publications on this topic. Tawfik [14] has presented a brief overview of the evolution of nanofluids in various applications. According to their research, nanotubes have higher thermal conductivity than spherical particles. Gowda et al. [15] analyze the effect of magnetic field on Casson-Maxwell nanofluid flow confined between two uniformly stretchable disks using the Buongiorno model. The outcomes showed that, in comparison to the Casson fluid, the Maxwell fluid is more strongly affected by the Lorentz force. Said et al. [16] presented a comparison of traditional and nanofluid-based thermal photovoltaics in terms of performance and environmental impact. They concluded that PV/T systems that employed nanofluid in any form, either coolant or filter, had higher overall exergy and energy efficiency than PV/T systems that used conventional fluid. A steady Maxwell model for nanofluid flow across a permeable stretched sheet containing gyrotactic microorganisms is explored by Safdar et al. [17]. Entropy production in a parabolic trough surface collector (PTSC) mounted inside a solar-powered ship using Maxwell nanofluids containing single wall carbon nanotube (SWCNTs) and multi-wall carbon nanotube (MWCNTs) is analyzed by Jamshed et al. [18]. Their results revealed that the thermal efficiency has boosted from 1.6% to 14.9% when SWCNTs compared to MWCNTs. Parvin et al. [19] constructed a 2D-double diffusive fluid model to analyze Brownian and thermophoretic diffusion on Maxwell fluid flow over an inclined sheet under the effect of magnetic field and suction. Jamshed et al. [18] analyzed the renewable solar energy by using Copper-methanol ($Cu-Ch_3OH$) and Titanium-methanol (TiO_2-Ch_3OH) in the Maxwell fluid moving over an infinite stretchable plate inside the PTSC. According to the results, $Cu-Ch_3OH$ nanofluid transfers heat more effectively than TiO_2-Ch_3OH. Some insightful discussions on the applications of nanofluids are addressed in references [20–23]

It is worth mentioning thermal conductivity of a nanoparticle plays a leading role in enhancing the efficacy of a thermal system. Among the metallic nanoparticles, gold (Au), silver (Ag), and copper (Cu) owned highest thermal conductivity. However, these particles are only available in restricted quantities because of their exorbitant price. Additionally, toxicity problems may stem from unmodified Au, Ag and Cu [24]. Although oxide nanoparticles are inexpensive, they have a lesser thermal conductivity than other nanomaterials. Using a novel fluid dubbed hybrid nanofluid, a combination of nanomaterials and nanofluid, these limitations can be overcome. Hybrid nanofluids offer synergy and advantageous thermal effects in contrast to ordinary fluids and nanofluids [25]. Entropy production in hybrid nanofluid flow over a stretchy surface in Darcy-Forchheimer medium with Marangoni convection was investigated by Khan et al. [26]. A two-phase model with modified Fourier heat flux law was used to investigate the impact of hybrid nanoparticles on the dusty fluid flow through a stretched cylinder [27, 28]. Li et al. [29] studied the consequences of viscous nonlinear convection and radiation on thermal and solutal Marangoni convection flow of Casson hybrid nanofluid flow over a spinning disc. Turcu et al. [30] may have been the first to describe the synthesis of crossover nano-composite particles, which included two distinct halves of PPY-CNT nano-composite and MWCNT on attractive Fe_3O_4 nanoparticles. Several aspects affecting heat transfer increases in hybrid nanofluids have been found, including nanoparticle synthesis, thermal conductivity, preparation process, particle level, nanoparticle compatibility, shape, and optimal thermal network development within fluids [31–36].

The aforementioned literature reveals that the studies UCM model using the notion of a frac-

tional derivative are rare. Therefore, this research aims to perform a numerical analysis of the fractional UCM viscoelastic hybrid nanofluid flow model with Cattaneo heat flux. The considered hybrid nanofluid is a mixture of MWCNTs-Al_2O_3 composite nanomaterials and mineral oil. The oxide nanoparticles Al_2O_3 is chosen because of its availability at a low cost. But the thermal conductivity of Al_2O_3 is not enough to acquire the desired heat transfer rates. On the other hand, many writers, on the other hand, have suggested increasing the thermal conductivity of nanofluids by selecting particles with higher thermal conductivity [14]. Therefore, MWCNTs have been added into Al_2O_3-mineral oil nanofluid to get better results. The appropriate quantities of alumina nanoparticle and MWCNTs are dispersed in mineral oil wiht a 90:10 proportion, respectively. The study has become more innovative by incorporating time-fractional derivatives into the UCM fluid model. Moreover, the previous studies on Maxwell fluid are solved using similarity transformation that transforms partial differential equations into ordinary differential equations. But this research solves partial differential equations using an unconditionally stable numerical method based on the Crank-Nicolson and L1 algorithm of the Caputo derivative. Investigations are conducted into how the relevant variables affect fluid properties, and the results are presented graphically and explored in depth.

2. Governing equations

The following continuity and momentum equations govern the flow of an incompressible anomalous Maxwell fluid [13]

$$\nabla \cdot V = 0, \tag{1}$$

$$\rho\left(\frac{\partial V}{\partial t} + V \cdot \nabla V\right) = \nabla \cdot \sigma. \tag{2}$$

Here V is the velocity field, ρ is the density of the fluid, and σ is the well known Cauchy stress tensor defined as

$$\sigma = -pI + \mathcal{T}, \tag{3}$$

where p represents hydor-static pressure, I denotes an identity matrix, and $\mathcal{T}$ refers to extra-stress tensor given as follows

$$\mathcal{T} + \lambda_1\left(\frac{\partial \mathcal{T}}{\partial t} + V \cdot \nabla \mathcal{T} - (\nabla V)\mathcal{T} - \mathcal{T}(\nabla V)^{\dagger}\right) = \mu \mathcal{A}_1. \tag{4}$$

Here † represents transpose of a matrix, λ_1 denotes time relaxation parameter, μ is the dynamic viscosity, and $\mathcal{A}_1$ is the first Rivlin–Erickson tensor defined as

$$\mathcal{A}_1 = \nabla V + (\nabla V)^{\dagger}, \tag{5}$$

A basic way for introducing fractional derivatives to linear viscoelasticity models is to replace the first derivative in the constitutive equation with a fractional derivative of order α. The fractional

expression of constitutive Equation (4) is

$$\mathcal{T} + \lambda_1^{\alpha}\left(\partial_t^{\alpha}\mathcal{T} + V \cdot \nabla\mathcal{T} - (\nabla V)\mathcal{T} - \mathcal{T}(\nabla V)^{\dagger}\right) = \mu\mathcal{A}_1. \tag{6}$$

The internal (thermal) energy balance law is as follows

$$\rho C_p\left(\frac{\partial T}{\partial t} + V \cdot \nabla T\right) = -\nabla \cdot q + \mathcal{T} : \nabla V. \tag{7}$$

The heat flux q is given by the Fourier law of heat conduction as follows

$$q = -k\Delta T, \tag{8}$$

where k is the thermal conductivity of the fluid. Several variations of Fourier's law have been offered. The most well-known of them is the Maxwell–Cattaneo law, defined as

$$\left(1 + \lambda_2\frac{\partial}{\partial t}\right)q = -k\nabla T. \tag{9}$$

Here λ_2 represents the thermal time relaxation parameter. In terms of time-fractional derivative of order β, the Maxwell–Cattaneo Equation (9) can be modified as

$$\left(1 + \lambda_2^{\beta}\partial_t^{\beta}\right)q = -k\nabla T. \tag{10}$$

3. Problem description

Consider a horizontal plate in the xz plane that is being surrounded by a Maxwell nanofluid. At first, the fluid is assumed to be at rest. Afterward, the mainstream flow is initiated due to an applied pressure gradient in the x direction

$$\frac{\partial p}{\partial x} = -\rho p_0\mathcal{H}(t), \tag{11}$$

where $\mathcal{H}$ indicates the Heaviside function, which has the following definition:

$$\mathcal{H}(t) = \begin{cases} 1, & t \geq 0, \\ 0, & t < 0. \end{cases} \tag{12}$$

Henceforth, the velocity field is assumed to be

$$V = \left(u(y, z, t), 0, 0\right). \tag{13}$$

Following that, the momentum Equation (2) reduced to

$$\rho\frac{\partial u}{\partial t} = -\frac{\partial p}{\partial x} + \frac{\partial \tau_{xy}}{\partial y} + \frac{\partial \tau_{xz}}{\partial z}. \tag{14}$$

Table 1
Thermal and physical attributes of base fluid and nanomaterials

Properties	Mineral oil	Al_2O_3	MWCNT
$\rho(kg/m^3)$	861	3970	2100
$k(W/mK)$	0.157	40	3000
$C_p(J/kgK)$	1860	765	710
μ (Pa.s)	0.01335	–	–

The constitution relation (6) gives us

$$\tau_{xy} + \lambda_1^{\alpha}\frac{\partial^{\alpha}\tau_{xy}}{\partial t^{\alpha}} = \mu\frac{\partial u}{\partial y}, \text{ and } \tau_{xz} + \lambda_1^{\alpha}\frac{\partial^{\alpha}\tau_{xz}}{\partial t^{\alpha}} = \mu\frac{\partial u}{\partial z}. \tag{15}$$

Eliminating τ_{xy} and τ_{xz} from Equations (14) and (15) results in

$$\rho\left(1 + \lambda_1^{\alpha}\partial_t^{\alpha}\right)\frac{\partial u}{\partial t} = \rho p_0\left(\mathcal{H}(t) + \lambda_1^{\alpha}\frac{t^{-\alpha}}{\Gamma(1-\alpha)}\right) + \mu\left(\frac{\partial^2 u}{\partial y^2} + \frac{\partial^2 u}{\partial z^2}\right). \tag{16}$$

Now, implementing the fractional Maxwell–Cattaneo Equation (10) together with Equation (13) to energy Equation (7) leads us to

$$\rho C_p\left(1 + \lambda_2^{\beta}\partial_t^{\beta}\right)\frac{\partial T}{\partial t} = k\left(\frac{\partial^2 T}{\partial y^2} + \frac{\partial^2 T}{\partial z^2}\right) + \tau_{xy}\frac{\partial u}{\partial y} + \tau_{xz}\frac{\partial u}{\partial z}. \tag{17}$$

4. Mathematical modeling for Maxwell hybrid nanofluid

To evaluate the effect of hybrid nanoparticles on fluid flow and heat transfer characteristics, it is obvious to introduce Maxwell hybrid nanofluid model. It is straightforward to replace the thermal and physical parameters of ordinary fluid with the equivalent attributes of hybrid nanofluid in Equations (16) and (17)

$$\rho_{hnf}\left(1 + \lambda_1^{\alpha}\partial_t^{\alpha}\right)\frac{\partial u}{\partial t} = \rho_{hnf} p_0\left(\mathcal{H}(t) + \lambda_1^{\alpha}\frac{t^{-\alpha}}{\Gamma(1-\alpha)}\right) + \mu_{hnf}\left(\frac{\partial^2 u}{\partial y^2} + \frac{\partial^2 u}{\partial z^2}\right). \tag{18}$$

$$\left(\rho C_p\right)_{hnf}\left(1 + \lambda_2^{\beta}\partial_t^{\beta}\right)\frac{\partial T}{\partial t} = k_{hnf}\left(\frac{\partial^2 T}{\partial y^2} + \frac{\partial^2 T}{\partial z^2}\right) + \left(1 + \lambda_2^{\beta}\partial_t^{\beta}\right)\left(\tau_{xy}\frac{\partial u}{\partial y} + \tau_{xz}\frac{\partial u}{\partial z}\right). \tag{19}$$

4.1. Thermal-physical attributes of hybrid nanofluid

Let φ_{p_1} and φ_{p_2} are the volume fraction of two different types of nanoparticles, and the subscripts f, nf, and hnf denote the base fluid, nanofluid and hybrid nanofluid, respectively. The mathematical expressions for thermal-physical attributes of nanofluid and hybrid nanofluid are given below [20, 26]

Density

The density of nanofluid ρ_{nf} in terms of ρ_f and φ_{p_1} can be define as

$$\rho_{nf} = (1-\varphi_{p_1})\rho_f + \varphi_{p_1}\rho_{p_1}. \tag{20}$$

The density of hybrid nanofluid may then be generated by altering the aforementioned density of nanofluid

$$\rho_{hnf} = (1-\varphi_{p_2})\rho_{nf} + \varphi_{p_2}\rho_{p_2}. \tag{21}$$

Dynamic viscosity

Below is an expression for nanofluid viscosity μ_{nf} in terms of base fluid viscosity μ_f and nanoparticles volume concentration φ_{p_1}

$$\mu_{nf} = \mu_f (1-\varphi_{p_1})^{-2.5}. \tag{22}$$

Modifying the above expression of viscosity (22) for hybrid nanofluid yield us to

$$\mu_{hnf} = \mu_f \left((1-\varphi_{p_1})(1-\varphi_{p_2}) \right)^{-2.5}. \tag{23}$$

Thermal conductivity

A relation between the thermal conductivities of nanofluid k_{nf} and regular base fluid k_f is

$$\frac{k_{nf}}{k_f} = \frac{(k_{p_1}+2k_f) + 2\varphi_{p_1}(k_{p_1}-k_f)}{(k_{p_1}+2k_f) - \varphi_{p_1}(k_{p_1}-k_f)}. \tag{24}$$

The above relation (24) helps us in obtaining the thermal conductivity of hybrid nanofluid k_{hnf}

$$k_{hnf} = \frac{(k_{p_2}+2k_{nf}) + 2\varphi_{p_2}(k_{p_2}-k_{nf})}{(k_{p_2}+2k_{nf}) - \varphi_{p_2}(k_{p_2}-k_{nf})} \times k_{nf}. \tag{25}$$

However, the thermal conductivity of CNT-hybrid nanofluid is provided as

$$k_{hnf} = \frac{1-\varphi_{p_2} + 2\varphi_{p_2}\dfrac{k_{p_2}}{k_{p_2}-k_{nf}} ln\dfrac{k_{p_2}+k_{nf}}{2k_{nf}}}{1-\varphi_{p_2} + 2\varphi_{p_2}\dfrac{k_{nf}}{k_{p_2}-k_{nf}} ln\dfrac{k_{p_2}+k_{nf}}{2k_{nf}}} \times k_{nf}. \tag{26}$$

Heat capacitance

If the heat capacitance of a nanofluid $(\rho C_p)_{nf}$ is provided as

$$(\rho C_p)_{nf} = (1-\varphi_{p_1})(\rho C_p)_f + \varphi_{p_1}(\rho C_p)_{p_1}. \tag{27}$$

Then the heat capacitance of hybrid nanofluid $(\rho C_p)_{hnf}$ can be written as

$$(\rho C_p)_{hnf} = (1-\varphi_{p_2})(\rho C_p)_{nf} + \varphi_{p_2}(\rho C_p)_{p_2} \tag{28}$$

5. Non-dimensional problem

This section is designed to introduce nano-dimensional parameters which will help us in obtaining the non-dimensional form of considering the Maxwell model. Below is a list of non-dimensional parameters

$$y^* = \frac{y}{z_{max}},\ z^* = \frac{z}{z_{max}},\ t^* = \frac{\nu_f t}{z_{max}^2},\ u^* = \frac{u z_{max}}{\nu_f},\ T^* = \frac{T-T_\infty}{q_w z_{max}/k_f},$$
$$\lambda_1^* = \frac{\lambda_1 \nu_f}{z_{max}^2},\ \lambda_2^* = \frac{\lambda_2 \nu_f}{z_{max}^2},\ \bar{\tau}_{xy}^* = \frac{z_{max}^2 \tau_{xy}}{\mu_f \nu_f},\ \tau_{xz}^* = \frac{z_{max}^2 \tau_{xz}}{\mu_f \nu_f}. \tag{29}$$

Invoking aforementioned parameters (29) in governing Equations (18) and (19) of Maxwell hybrid nanofluid model and removing $*$ for simplicity yields us to

$$a_1\left(1+\lambda_1^\alpha \partial_t^\alpha\right)\frac{\partial u}{\partial t} = a_1 p_0\left(\mathcal{H}(t) + \lambda_1^\alpha \frac{t^{-\alpha}}{\Gamma(1-\alpha)}\right) + a_2\left(\frac{\partial^2 u}{\partial y^2} + \frac{\partial^2 u}{\partial z^2}\right). \tag{30}$$

$$a_3 Pr\left(1+\lambda_2^\beta \partial_t^\beta\right)\frac{\partial T}{\partial t} = a_4\left(\frac{\partial^2 T}{\partial y^2} + \frac{\partial^2 T}{\partial z^2}\right) + \mathcal{E}\left(1+\lambda_2^\beta \partial_t^\beta\right)\left(\tau_{xy}\frac{\partial u}{\partial y} + \tau_{xz}\frac{\partial u}{\partial z}\right). \tag{31}$$

Given that

$$p = \frac{p_0 z_{max}^3}{\nu_f^2},\ \mathcal{E} = \frac{\mu_f \nu_f^2}{q_w z_{maz}^3},\ Pr = \frac{\mu_f C_{p_f}}{k_f}, a_1 = \left(1-\varphi_{p_2}\right)\frac{\rho_{nf}}{\rho_f} + \varphi_{p_2}\frac{\rho_{p_2}}{\rho_f},$$
$$a_2 = \left((1-\varphi_{p_1})(1-\varphi_{p_2})\right)^{-2.5},\ a_3 = \left(1-\varphi_{p_2}\right)\frac{(\rho C_p)_{nf}}{(\rho C_p)_f} + \varphi_{p_2}\frac{(\rho C_p)_{p_2}}{(\rho C_p)_f},\ a_4 = \frac{k_{hnf}}{k_f}. \tag{32}$$

The non-dimensional initial and boundary conditions are

$$\begin{cases} u(y,z,t) = 0 = \dfrac{\partial u(y,z,t)}{\partial t}, \; T(y,z,t) = 0, t < 0, \; (y,z) \in [0,\infty) \times [0, z_{max}], \\ u(0,z,t) = 0, \; a_4 \dfrac{\partial T(0,z,t)}{\partial y} = -1, \; t > 0, \; z \in [0, z_{max}], \\ u(y,0,t) = 0 = u(y, z_{max}, t), \; T(y,0,t) = 0 = T(y, z_{max}, t), \; t > 0, \; y \in [0,\infty), \\ u(y,z,t) \to 0, \; T(y,z,t) \to 0 \text{ as } y \to \infty. \end{cases} \tag{33}$$

6. Heat transfer coefficient

The Nusselt number commonly referred to as the heat transfer coefficient, is a measure of heat transport in a thermal system. The definition of it in mathematics is [37]

$$Nu_l = \frac{z q_w}{k_f (T_w - T_\infty)}, \tag{34}$$

here $q_w = -k_{nf}\left(\dfrac{\partial T}{\partial y}\right)_{y=0}$ refers to wall heat flux, the fractional form is appended below [3]

$$\left(1 + \lambda_2^\beta \partial_t^\beta\right) q_w = -k_{nf}\left(\frac{\partial T}{\partial y}\right)_{y=0}. \tag{35}$$

Operating $\left(1 + \lambda_2^\beta \partial_t^\beta\right)$ on both side of Equation (34) and using the non-dimensional parameters (29) and the fractional form of q_w (35), we arrived at

$$\left(1 + \lambda_2^\beta \partial_t^\beta\right) Nu_L = \frac{-z a_4 \left(\dfrac{\partial T}{\partial y}\right)_{y=0}}{T(0)}. \tag{36}$$

7. Numerical approximation

This section presents the numerical approximation for the non-dimensional Equations (30) and (31). An implicit finite difference method, namely the Crank–Nicolson method will be used to approximate the integer-order derivatives, whereas fractional-order time derivatives will be approximated using Caputo fractional derivative.

Define $y_i = i\Delta y, i = 1, 2, \cdots, l$, $z_j = j\Delta z, j = 1, 2, \cdots, m$, where $\Delta y = y_{max}/l$, and $\Delta z = z_{max}/m$ are the mesh size in (y, z) direction. Let $t_k = k\Delta t, k = 0, 1, \cdots, n$ with the time step $\Delta t = t_f/n$. We will use the following approximations for derivatives from now on:

- Integer-order derivatives

$$\left.\frac{\partial u}{\partial t}\right|_{t_k} = \frac{u_{i,j}^{k} - u_{i,j}^{k-1}}{\Delta t}, \quad \left.\frac{\partial T}{\partial t}\right|_{t_k} = \frac{T_{i,j}^{k} - T_{i,j}^{k-1}}{\Delta t}. \tag{37}$$

$$\left.\frac{\partial u}{\partial y}\right|_{t_k} = \frac{u_{i+1,j}^{k} - u_{i,j}^{k} + u_{i+1,j}^{k-1} - u_{i,j}^{k-1}}{2\Delta y}. \tag{38}$$

$$\left.\frac{\partial u}{\partial z}\right|_{t_k} = \frac{u_{i,j+1}^{k} - u_{i,j-1}^{k} + u_{i,j+1}^{k-1} - u_{i,j-1}^{k-1}}{4\Delta z}. \tag{39}$$

$$\left.\frac{\partial^2 u}{\partial y^2}\right|_{t_k} = \frac{u_{i-1,j}^{k} - 2u_{i,j}^{k} + u_{i+1,j}^{k} + u_{i-1,j}^{k-1} - 2u_{i,j}^{k-1} + u_{i+1,j}^{k-1}}{2\Delta y}. \tag{40}$$

$$\left.\frac{\partial^2 u}{\partial z^2}\right|_{t_k} = \frac{u_{i,j-1}^{k} - 2u_{i,j}^{k} + u_{i,j+1}^{k} + u_{i,j-1}^{k-1} - 2u_{i,j}^{k-1} + u_{i,j+1}^{k-1}}{2\Delta z}. \tag{41}$$

$$\left.\frac{\partial^2 T}{\partial y^2}\right|_{t_k} = \frac{T_{i-1,j}^{k} - 2T_{i,j}^{k} + T_{i+1,j}^{k} + T_{i-1,j}^{k-1} - 2T_{i,j}^{k-1} + T_{i+1,j}^{k-1}}{2\Delta y^2}. \tag{42}$$

$$\left.\frac{\partial^2 T}{\partial z^2}\right|_{t_k} = \frac{T_{i,j-1}^{k} - 2T_{i,j}^{k} + T_{i,j+1}^{k} + T_{i,j-1}^{k-1} - 2T_{i,j}^{k-1} + T_{i,j+1}^{k-1}}{2\Delta z^2}. \tag{43}$$

- Fractional-order derivatives

$$\left.\frac{\partial^{\alpha+1} u}{\partial t^{\alpha+1}}\right|_{t_k} = \frac{\Delta t^{-\alpha-1}}{\Gamma(2-\alpha)}\left(u_{i,j}^{k} - u_{i,j}^{k-1} - \sum_{s=1}^{k-1} b_s\left(u_{i,j}^{k-s} - u_{i,j}^{k-s-1}\right)\right). \tag{44}$$

$$\left.\frac{\partial^{\beta+1} T}{\partial t^{\beta+1}}\right|_{t_k} = \frac{\Delta t^{-\beta-1}}{\Gamma(2-\beta)}\left(T_{i,j}^{k} - T_{i,j}^{k-1} - \sum_{r=1}^{k-1} d_r\left(T_{i,j}^{k-r} - T_{i,j}^{k-r-1}\right)\right). \tag{45}$$

$$\frac{\partial^{\beta}}{\partial t^{\beta}}\left(\tau_{xy}\frac{\partial u}{\partial y}\right)\Big|_{t_k} = \frac{\Delta t^{-\beta}}{4\Delta y\Gamma(2-\beta)}\Bigg(\left(\tau_{xy}^{k}+\tau_{xy}^{k-1}\right)\left(u_{i+1,j}^{k}-u_{i,j}^{k}+u_{i+1,j}^{k-1}-u_{i,j}^{k-1}\right)$$

$$-\sum_{r=1}^{k-1} d_r\left(\tau_{xy}^{k}+\tau_{xy}^{k-1}\right)\left(u_{i+1,j}^{k-r}-u_{i,j}^{k-r}-u_{i+1,j}^{k-r-1}-u_{i,j}^{k-r-1}\right)\Bigg). \tag{46}$$

$$\frac{\partial^{\beta}}{\partial t^{\beta}}\left(\tau_{xz}\frac{\partial u}{\partial z}\right)\Big|_{t_k} = \frac{\Delta t^{-\beta}}{8\Delta z\Gamma(2-\beta)}\Bigg(\left(\tau_{xz}^{k}+\tau_{xz}^{k-1}\right)\left(u_{i,j+1}^{k}-u_{i,j-1}^{k}+u_{i,j+1}^{k-1}-u_{i,j-1}^{k-1}\right)$$

$$-\sum_{r=1}^{k-1} d_r\left(\tau_{xy}^{k}+\tau_{xy}^{k-1}\right)\left(u_{i,j+1}^{k-r}-u_{i,j-1}^{k-r}+u_{i,j+1}^{k-r-1}-u_{i,j-1}^{k-r-1}\right)\Bigg). \tag{47}$$

Note that $b_s = (a_{s-1} - a_s)$ and $d_r = (c_{r-1} - c_r)$. Let us introduce

$$c_1 = \frac{a_2}{a_1},\ c_2 = \frac{a_4}{a_3},\ c_3 = \frac{\Delta t}{2\Delta y^2},\ c_4 = \frac{\Delta t}{2\Delta z^2},\ E_1 = \frac{p_0\Delta t}{2},\ E_2 = c_1c_3,\ E_3 = c_1c_4,\ E_4 = \frac{c_2c_3}{Pr},$$

$$E_5 = \frac{c_2c_4}{Pr},\ E_6 = \frac{c_3\Delta y\mathcal{E}\left(1+\delta_2\right)}{2a_3Pr},\ E_7 = \frac{c_4\Delta z\mathcal{E}\left(1+\delta_2\right)}{4a_3Pr},\ \delta_1 = \frac{\lambda_1^{\alpha}\Delta t^{-\alpha}}{\Gamma(2-\alpha)},\ \delta_2 = \frac{\lambda_2^{\beta}\Delta t^{-\beta}}{\Gamma(2-\beta)}. \tag{48}$$

Using Equations (37)–(48) in Equations (30) and (31), we arrived at

$$\left(1+\delta_1\right)\left(u_{i,j}^{k}-u_{i,j}^{k-1}\right) = E_1\left(\mathcal{H}(t_k)+\mathcal{H}(t_{k-1})+\lambda_1^{\alpha}\frac{t_k^{-\alpha}+t_{k-1}^{-\alpha}}{\Gamma(1-\alpha)}\right)+E_2\Big(u_{i-1,j}^{k}-2u_{i,j}^{k}$$

$$+u_{i+1,j}^{k}+u_{i-1,j}^{k-1}-2u_{i,j}^{k-1}+u_{i+1,j}^{k-1}\Big)+E_3\Big(u_{i,j-1}^{k}-2u_{i,j}^{k} \tag{49}$$

$$+u_{i,j+1}^{k}+u_{i,j-1}^{k-1}-2u_{i,j}^{k-1}+u_{i,j+1}^{k-1}\Big)+\delta_1\mathrm{P}[A_1],$$

$$\left(1+\delta_2\right)\left(T_{i,j}^{k}-T_{i,j}^{k-1}\right)=E_4\left(T_{i-1,j}^{k}-2T_{i,j}^{k}+T_{i+1,j}^{k}+T_{i,j+1}^{k-1}-2T_{i,j}^{k-1}+T_{i,j}^{k-1}\right)$$

$$+E_5\left(T_{i,j-1}^{k}-2T_{i,j}^{k}+T_{i,j+1}^{k}+T_{i,j-1}^{k-1}-2T_{i,j}^{k-1}+T_{i,j+1}^{k-1}\right)$$

$$+E_6\left(\tau_{xy}^{k}+\tau_{xy}^{k-1}\right)\left(u_{i+1,j}^{k}-u_{i,j}^{k}+u_{i+1,j}^{k-1}-u_{i,j}^{k-1}\right) \tag{50}$$

$$+E_7\left(\tau_{xz}^{k}+\tau_{xz}^{k-1}\right)\left(u_{i,j+1}^{k}-u_{i,j-1}^{k}+u_{i,j+1}^{k-1}-u_{i,j-1}^{k-1}\right)$$

$$+\delta_2\left(\text{Þ}[A_2]-E_6\text{Þ}[A_3]-E_7\text{Þ}[A_4]\right).$$

Provided that

$$\text{Þ}[A_1]=\sum_{s=1}^{k-1}b_s\left(u_{i,j}^{k-s}-u_{i,j}^{k-s-1}\right),\ \text{Þ}[A_2]=\sum_{r=1}^{k-1}d_r\left(T_{i,j}^{k-r}-T_{i,j}^{k-r-1}\right),$$

$$\text{Þ}[A_3]=\left(1+\delta_2\right)^{-1}\sum_{r=1}^{k-1}d_r\left(\tau_{xy}^{k-r}+\tau_{xy}^{k-r-1}\right)\left(u_{i+1,j}^{k-r}-u_{i,j}^{k-r}+u_{i+1,j}^{k-r-1}-u_{i,j}^{k-r-1}\right), \tag{51}$$

$$\text{Þ}[A_4]=\left(1+\delta_2\right)^{-1}\sum_{r=1}^{k-1}d_r\left(\tau_{xz}^{k-r}+\tau_{xz}^{k-r-1}\right)\left(u_{i,j+1}^{k-r}-u_{i,j-1}^{k-r}+u_{i,j+1}^{k-r-1}-u_{i,j-1}^{k-r-1}\right).$$

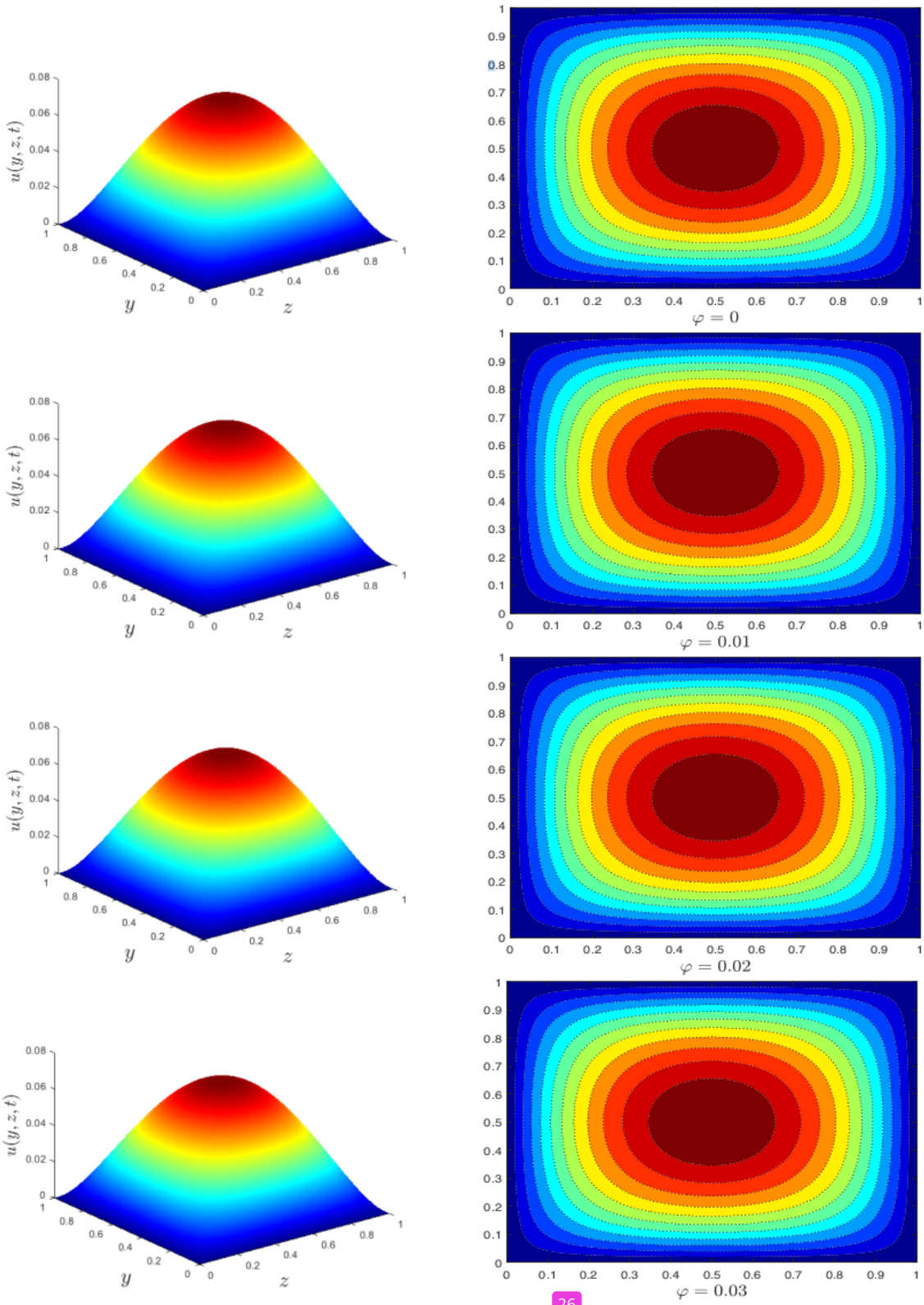

Figure 1: Velocity profile for different values of nanoparticle volume fraction φ

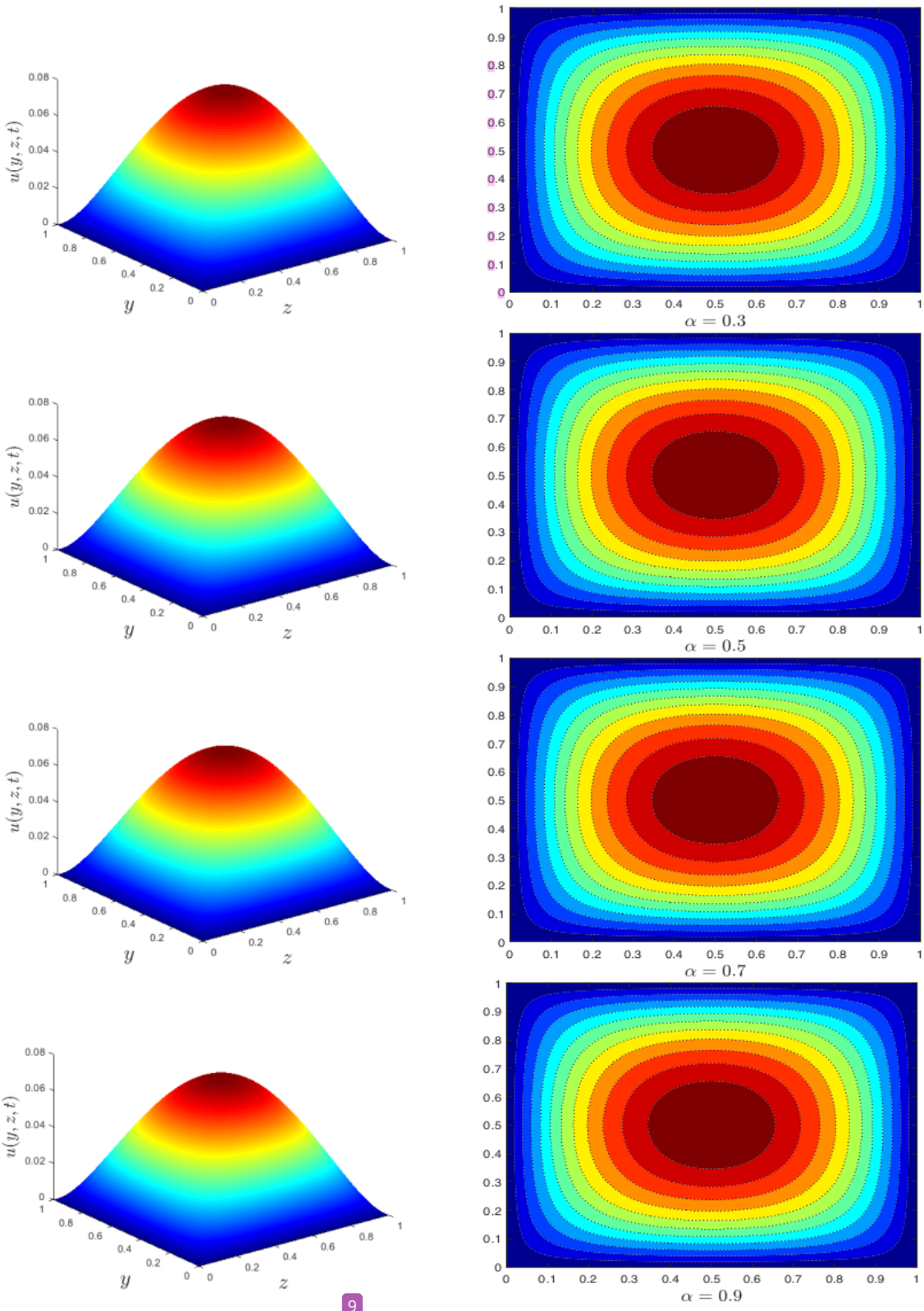

Figure 2: Velocity profile for different values of fractional derivative parameter α

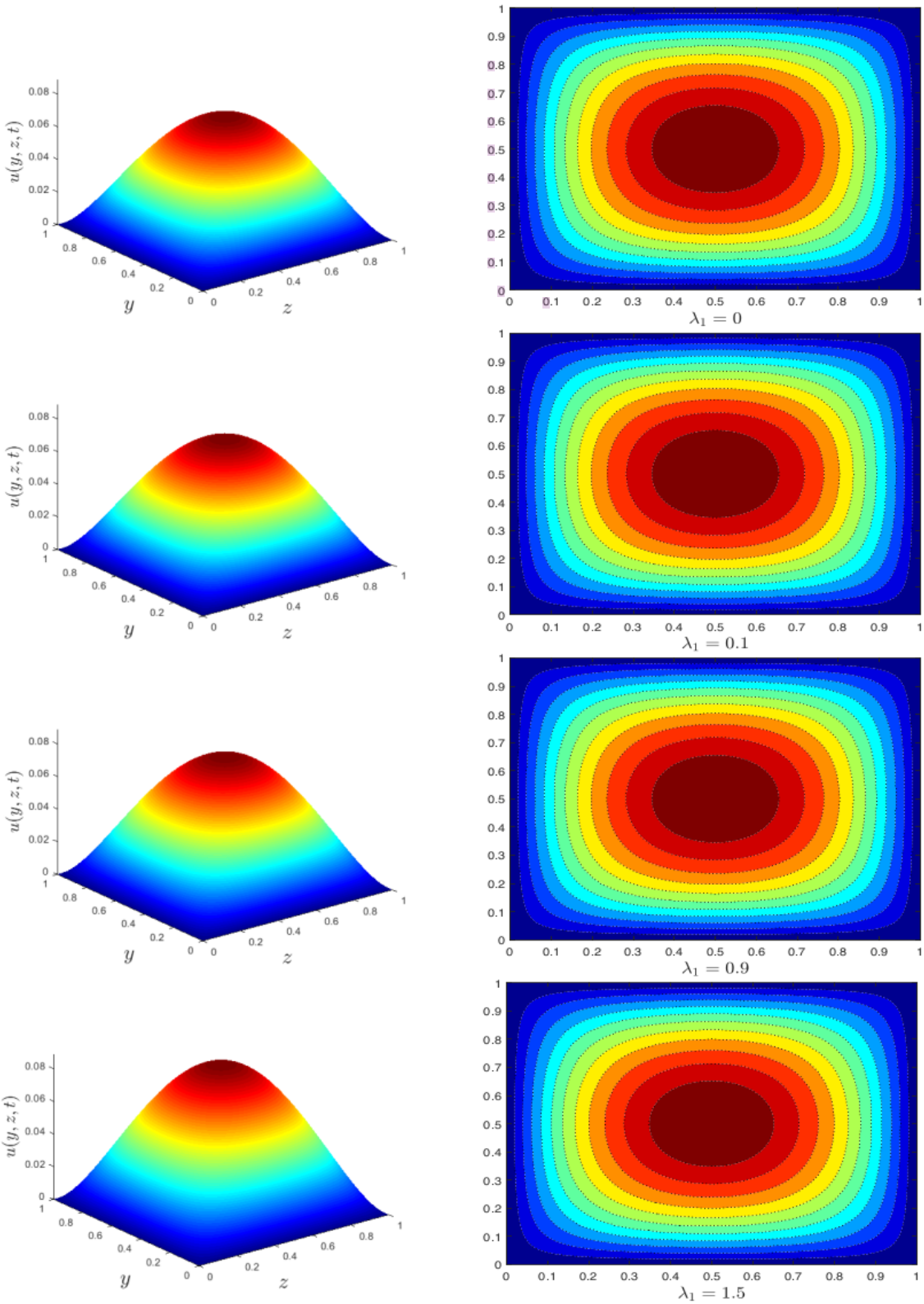

Figure 3: Velocity profile for different values of relaxation time λ_1

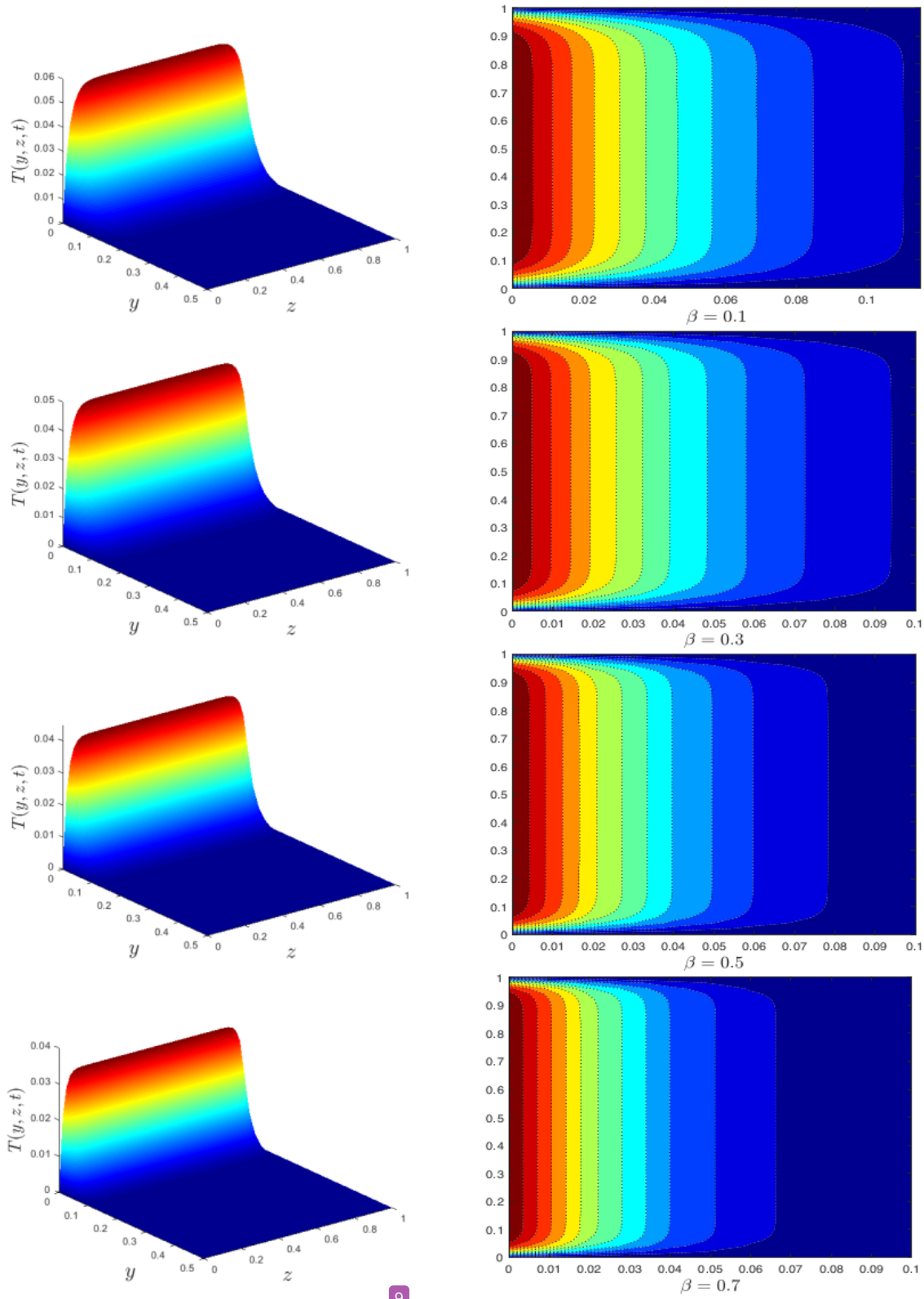

Figure 4: Temperature profile for different values of fractional derivative parameter β

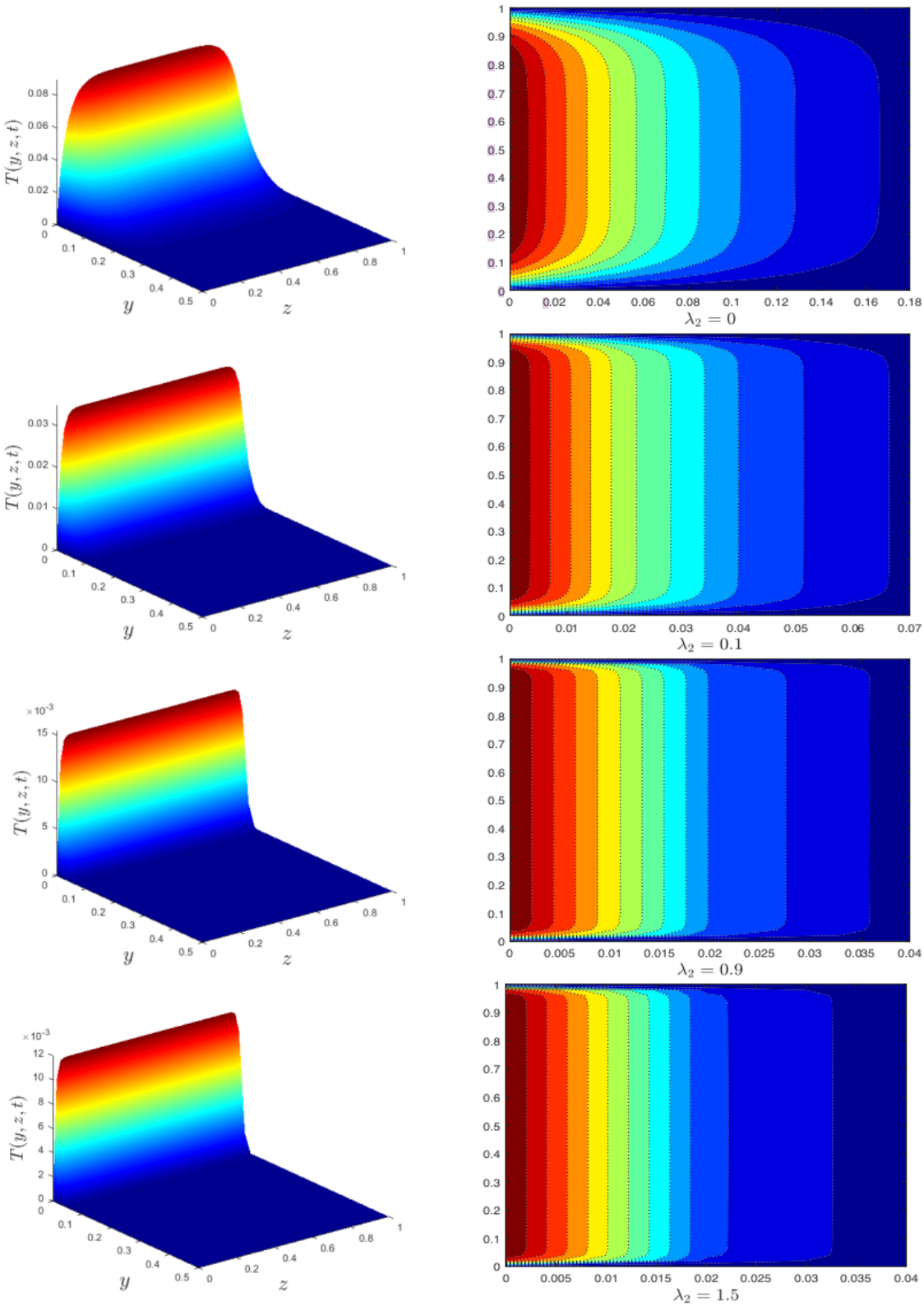

Figure 5: Temperature profile for different values of relaxation time λ_2

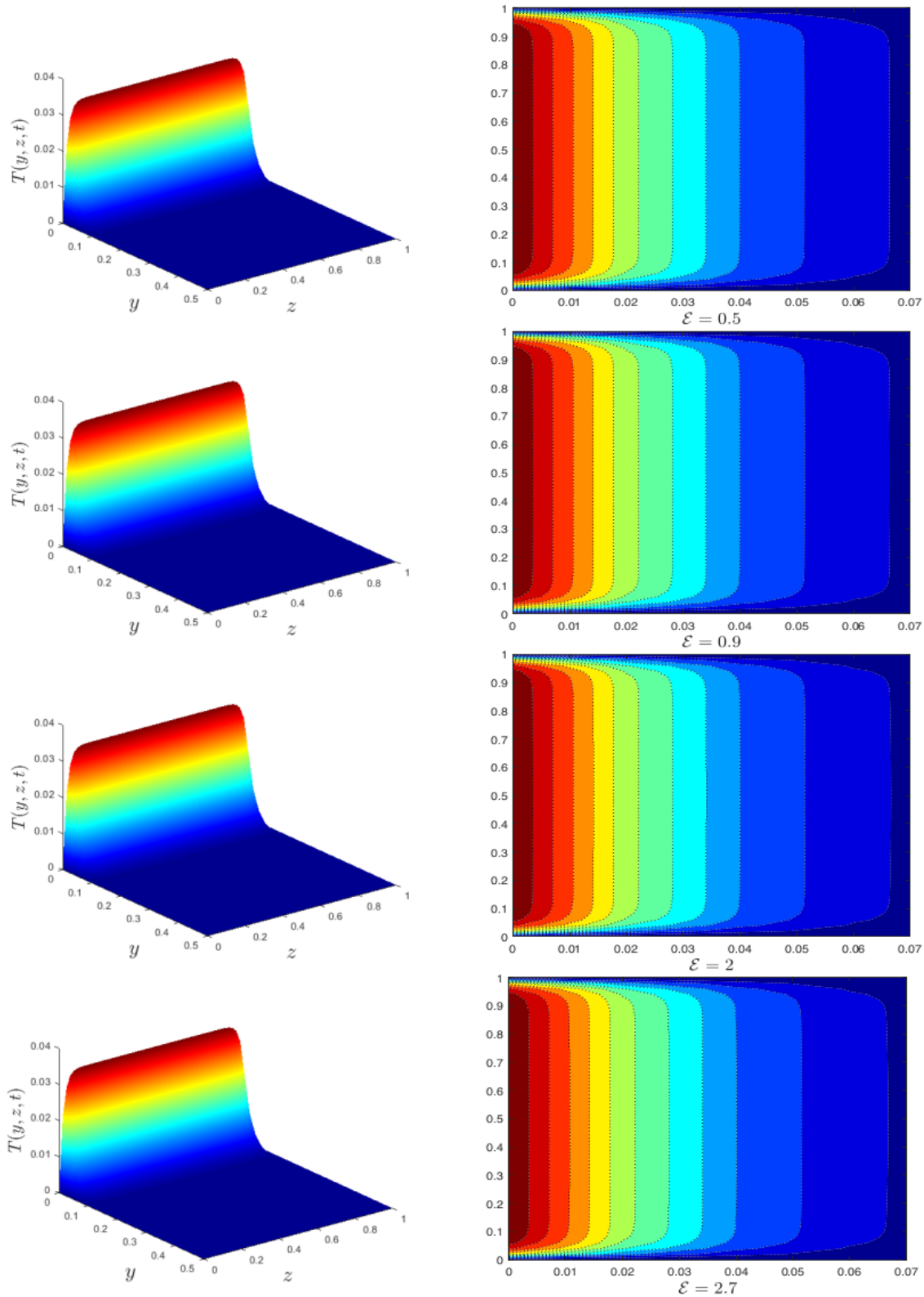

Figure 6: Temperature profile for different values of dissipation parameter $\mathcal{E}$

8. Results and discussion

The purpose of this part is to help to understand the explanation of the graphical illustrations. This part will go over the theoretical components of the problem, such as nanomaterials volume fraction, fractional-order derivative, relaxation time and viscous dissipation. To attain this goal, the MATLAB software is used to solve the discrete governing equations Equations (49) and (50). Figures 1–10 are intended to determine the effect of all governing parameters on fluid flow and heat transfer characteristics. The parameters are considered to have the following fixed numerical values: $\varphi = \varphi_{p_1} + \varphi_{p_2} = 0.01, \mathcal{E} = 0.5, \alpha = 0.7 = \beta$, and $\lambda_1 = 0.1 = \lambda_2$, unless otherwise stated.

To begin, the numerical computations in Figure 1 are performed to determine the impact of the nanomaterial volume fraction on the velocity field. This figure evidenced a decrement in fluid flow velocity on adding nanomaterials. The fluid becomes more viscous as the concentration of particles inside the fluid increases, which causes a drop in velocity flow.

Figure 2 shows features of the fractional derivative parameter α on the velocity field. The fractional derivative α not only quantifies the frequency-dependent complex modulus but also anticipates the relaxation and creep-responses of viscoelastic fluid [38]. The velocity field declines when α increases. One may anticipate, that as α increases, the resistance of the material particles increases. which decreases the flow speed. Figure 3 depicts the consequences of the relaxation time parameter λ_1 on the velocity profile of the fluid. According to Figure 3, which illustrates the delaying property of viscoelastic fluid, the more the relaxation time parameter the more the velocity of the fluid. The length of time needed to return to normal condition grows as λ_1 increases, which results in an increase in the velocity field.

The fluctuation in the non-dimensional temperature with different values of the fractional derivative parameter β can be observed in the Figure 4. The fractional derivative parameter β might be a new indicator of heat conduction in a conducting material. An appropriate value of β can increase the effectiveness of a thermo-electric material figure-of-merit [39].The temperature profile diminishes as β increases. Increasing the magnitude of β can obstruct the temperature distribution. Drawing Figure 5 is an effort to conjure up the relation between temperature and relaxation time parameter λ_2. This resolves the paradox of unbounded heat propagation speed in thermo-electric fluid [40]. The temperature profile diminishes as the value of λ_2 rises. Figure 6 shows the relationship between the viscous dissipation $\mathcal{E}$ and the temperature of Maxwell hybrid nanofluid. As Ec rises, the fluid's capacity to retain heat energy increases due to friction forces, improving the temperature profile.

Next, the effects of various embedded elements on the surface temperature are sketched out in Figures 7 and 8. The fluid temperature on the surface of the plate decreases for high volume concentration, see Figure 7. Generally, the increased volume of nanomaterials improves the thermal conductivity of a fluid. However, several factors affect fluid's thermal conductivity, including the nanomaterials concentration, compatibility, preparation process, type, shape, and composition of the nanoparticles. On the other hand, the wall temperature increases due to the viscous dissipation effect. Figure 8 shows that the surface temperature is a decreasing function of fractional derivative and relaxation time parameters.

Finally, we arrived at column graphs Figures 9 and 10 at this point, depict the variation of the Nusselt number in response to various pertinent parameters. It can be seen in Figure 9 that the maximum Nusselt number is owned on increasing nanomaterial volume concentration. It is

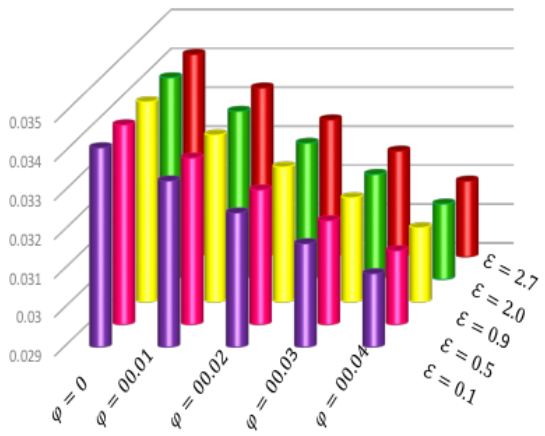

Figure 7: Impact of dissipation parameter $\mathcal{E}$ and nanomaterial volume fraction φ on $T(0)$

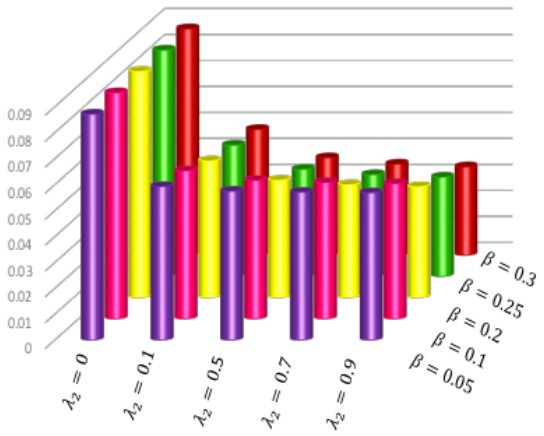

Figure 8: Impact of fractional parameter β and relaxation time λ_2 on $T(0)$

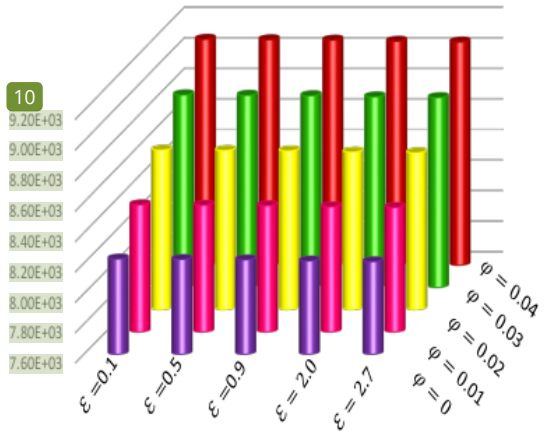

Figure 9: Impact of dissipation parameter $\mathcal{E}$ and nanomaterial volume fraction φ on Nu_L

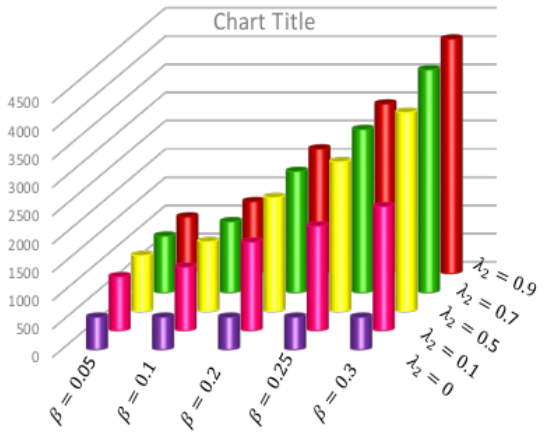

Figure 10: Impact of fractional parameter β and relaxation time λ_2 on Nu_L

closed to physical expectations as the thermal conductivity of the fluid increases on interacting with nanomaterials. Moreover, the Nusselt number decreases abruptly for increasing values of the viscous dissipation parameter. Drawing Figure 10 is an effort to conjure up the influences of fractional derivative β and relaxation time parameter λ_2 on the surface temperature of Maxwell hybrid nanofluid. It is observed that the Nusselt number is an increasing function of fractional derivative and relaxation time parameters.

9. Conclusions

This research is conducted to evaluate the MWCNTs-Al_2O_3 nanomaterials, viscous dissipation, fractional derivatives, and their impact on flow and heat transfer characteristics of Maxwell nanofluid. The fractional UCM model is solved using the Caputo derivative and the Crank-Nicolson method. Below is a list of the main affirmative aspects:

- The less the nanomaterial volume concentration and fractional derivative parameter the more

the velocity of Maxwell hybrid nanofluid.

- To manifest a surface heat increase, the nanomaterial concentration, the fractional derivative parameter, and the relaxation time parameter must all be modest.
- At high levels of the relaxation time, fractional derivative, and nanomaterial concentration parameters, Nusselt number augmentation may be projected.
- In general, when $\varphi = 0 = \lambda 1$, it is possible to predict the Maxwell fluid flow.

It is envisaged that other hybrid flow models will draw ideas from the current work. It is uncommon to find a flow configuration that includes a fractional time derivative and the hypothesis of a hybrid nanofluid. Therefore, a number of industrial and engineering issues may be resolved with the aid of this study.

References

[1] C. W. Mackosko, Rheology: principles, measurements and applications, 1994. https://www.wiley.com/en-us/exportProduct/pdf/9780471185758.

[2] K. S. Adegbie, A. J. Omowaye, A. B. Disu, I. L. Animasaun, et al., Heat and mass transfer of upper convected Maxwell fluid flow with variable thermo-physical properties over a horizontal melting surface, Applied Mathematics 6 (2015) 1362. https://doi.org/10.4236/am.2015.68129.

[3] H. Hanif, Cattaneo–friedrich and crank–nicolson analysis of upper-convected Maxwell fluid along a vertical plate, Chaos, Solitons & Fractals 153 (2021) 111463. https://doi.org/10.1016/j.chaos.2021.111463.

[4] A. Omowaye, I. Animasaun, Upper-convected Maxwell fluid flow with variable thermo-physical properties over a melting surface situated in hot environment subject to thermal stratification, Journal of Applied Fluid Mechanics 9 (2016) 1777–1790. https://doi.org/10.18869/acadpub.jafm.68.235.24939.

[5] R. N. Kumar, A. Jyothi, H. Alhumade, R. P. Gowda, M. M. Alam, I. Ahmad, M. Gorji, B. Prasannakumara, Impact of magnetic dipole on thermophoretic particle deposition in the flow of Maxwell fluid over a stretching sheet, Journal of Molecular Liquids 334 (2021) 116494. https://doi.org/10.1016/j.molliq.2021.116494.

[6] R. Hilfer, Applications of fractional calculus in physics, World scientific, 2000. https://www.worldscientific.com/worldscibooks/10.1142/3779.

[7] F. Meral, T. Royston, R. Magin, Fractional calculus in viscoelasticity: an experimental study, Communications in nonlinear science and numerical simulation 15 (2010) 939–945. https://doi.org/10.1016/j.cnsns.2009.05.004.

[8] P. Yang, Y. C. Lam, K.-Q. Zhu, Constitutive equation with fractional derivatives for the generalized UCM model, Journal of Non-Newtonian Fluid Mechanics 165 (2010) 88–97. https://doi.org/10.1016/j.jnnfm.2009.10.002.

[9] M. Dalir, M. Bashour, Applications of fractional calculus, Applied Mathematical Sciences 4 (2010) 1021–1032. https://www.semanticscholar.org/paper/Applications-of-Fractional-Calculus-Dalir-Bashour/b9f3cebf62c66c7bc06eab009aa1d60d70a19312.

[10] H. Sun, Y. Zhang, D. Baleanu, W. Chen, Y. Chen, A new collection of real world applications of fractional calculus in science and engineering, Communications in Nonlinear Science and Numerical Simulation 64 (2018) 213–231. https://doi.org/10.1016/j.cnsns.2018.04.019.

[11] N. Sene, Analytical solutions and numerical schemes of certain generalized fractional diffusion models, The European Physical Journal Plus 134 (2019) 199. https://doi.org/10.1140/epjp/i2019-12531-4.

[12] N. Sene, Second-grade fluid model with caputo–liouville generalized fractional derivative, Chaos, Solitons & Fractals 133 (2020) 109631. https://doi.org/10.1016/j.chaos.2020.109631.

[13] H. Hanif, A computational approach for boundary layer flow and heat transfer of fractional Maxwell fluid, Mathematics and Computers in Simulation 191 (2022) 1–13. https://doi.org/10.1016/j.matcom.2021.07.024.

[14] M. M. Tawfik, Experimental studies of nanofluid thermal conductivity enhancement and applications: A review, Renewable and Sustainable Energy Reviews 75 (2017) 1239–1253. https://doi.org/10.1016/j.rser.2016.11.111.

[15] R. Gowda, A. Rauf, R. Naveen Kumar, B. Prasannakumara, S. Shehzad, Slip flow of casson–Maxwell nanofluid confined through stretchable disks, Indian Journal of Physics 96 (2022) 2041–2049. https://doi.org/10.1007/s12648-021-02153-7.

[16] Z. Said, S. Arora, E. Bellos, A review on performance and environmental effects of conventional and nanofluid-based thermal photovoltaics, Renewable and Sustainable Energy Reviews 94 (2018) 302–316. https://doi.org/10.1016/j.rser.2018.06.010.

[17] R. Safdar, M. Jawad, S. Hussain, M. Imran, A. Akgül, W. Jamshed, Thermal radiative mixed convection flow of mhd Maxwell nanofluid: Implementation of buongiorno's model, Chinese Journal of Physics 77 (2022) 1465–1478. https://doi.org/10.1016/j.cjph.2021.11.022.

[18] W. Jamshed, C. Şirin, F. Selimefendigil, M. Shamshuddin, Y. Altowairqi, M. R. Eid, Thermal characterization of coolant Maxwell type nanofluid flowing in parabolic trough solar collector (ptsc) used inside solar powered ship application, Coatings 11 (2021) 1552. https://doi.org/10.3390/coatings11121552.

[19] S. Parvin, S. S. P. M. Isa, W. Jamshed, R. W. Ibrahim, K. S. Nisar, Numerical treatment of 2d-magneto double-diffusive convection flow of a Maxwell nanofluid: Heat transport case study, Case Studies in Thermal Engineering 28 (2021) 101383. https://doi.org/10.1016/j.csite.2021.101383.

[20] W. Jamshed, Numerical investigation of MHD impact on Maxwell nanofluid, International Communications in Heat and Mass Transfer 120 (2021) 104973. https://doi.org/10.1016/j.icheatmasstransfer.2020.104973.

[21] H. Hanif, I. Khan, S. Shafie, MHD natural convection in cadmium telluride nanofluid over a vertical cone embedded in a porous medium, Physica Scripta 94 (2019) 125208. https://doi.org/10.1088/1402-4896/ab36e1.

[22] A. Aziz, W. Jamshed, T. Aziz, Mathematical model for thermal and entropy analysis of thermal solar collectors by using Maxwell nanofluids with slip conditions, thermal radiation and variable thermal conductivity, Open Physics 16 (2018) 123–136. https://doi.org/10.1515/phys-2018-0020.

[23] W. Jamshed, F. Shahzad, R. Safdar, T. Sajid, M. R. Eid, K. S. Nisar, Implementing renewable solar energy in presence of Maxwell nanofluid in parabolic trough solar collector: a computational study, Waves in Random and Complex Media (2021) 1–32. https://doi.org/10.1080/17455030.2021.1989518.

[24] K. Parveen, V. Banse, L. Ledwani, Green synthesis of nanoparticles: their advantages and disadvantages, in: AIP conference proceedings, volume 1724, AIP Publishing LLC, p. 020048. https://doi.org/10.1063/1.4945168.

[25] S. Salman, A. A. Talib, S. Saadon, M. H. Sultan, Hybrid nanofluid flow and heat transfer over backward and forward steps: A review, Powder Technology 363 (2020) 448–472. https://doi.org/10.1016/j.powtec.2019.12.038.

[26] M. I. Khan, S. Qayyum, F. Shah, R. N. Kumar, R. P. Gowda, B. Prasannakumara, Y.-M. Chu, S. Kadry, Marangoni convective flow of hybrid nanofluid (mnznfe2o4-niznfe2o4-h2o) with darcy forchheimer medium, Ain Shams Engineering Journal 12 (2021) 3931–3938. https://doi.org/10.1016/j.asej.2021.01.028.

[27] R. Varun Kumar, R. Punith Gowda, R. Naveen Kumar, M. Radhika, B. Prasannakumara, Two-phase flow of dusty fluid with suspended hybrid nanoparticles over a stretching cylinder with modified fourier heat flux, SN Applied Sciences 3 (2021) 1–9. https://doi.org/10.1007/s42452-021-04364-3.

[28] R. Punith Gowda, R. Naveen Kumar, B. Prasannakumara, Two-phase darcy-forchheimer flow of dusty hybrid nanofluid with viscous dissipation over a cylinder, International Journal of Applied and Computational Mathematics 7 (2021) 1–18. https://doi.org/10.1007/s40819-021-01033-2.

[29] Y.-X. Li, M. I. Khan, R. P. Gowda, A. Ali, S. Farooq, Y.-M. Chu, S. U. Khan, Dynamics of aluminum oxide and copper hybrid nanofluid in nonlinear mixed marangoni convective flow with entropy generation: Applications to renewable energy, Chinese Journal of Physics 73 (2021) 275–287. https://doi.org/10.1016/j.cjph.2021.06.004.

[30] R. Turcu, A. Darabont, A. Nan, N. Aldea, D. Macovei, D. Bica, L. Vekas, O. Pana, M. Soran, A. Koos, et al., New polypyrrole-multiwall carbon nanotubes hybrid materials, Journal of optoelectronics and advanced materials 8 (2006) 643–647. https://www.researchgate.net/publication/266224651_New_polypyrrole-multiwall_carbon_nanotubes_hybrid_materials.

[31] H. Hanif, I. Khan, S. Shafie, W. A. Khan, Heat transfer in cadmium telluride-water nanofluid over a vertical cone under the effects of magnetic field inside porous medium, Processes 8 (2019) 7.

[32] J. Madhukesh, R. N. Kumar, R. P. Gowda, B. Prasannakumara, G. Ramesh, M. I. Khan, S. U. Khan, Y.-M. Chu, Numerical simulation of aa7072-aa7075/water-based hybrid nanofluid flow over a curved stretching sheet with Newtonian heating: A non-Fourier heat flux model approach, Journal of Molecular Liquids 335 (2021) 116103. https://doi.org/10.1016/j.molliq.2021.116103.

[33] H. Hanif, I. Khan, S. Shafie, A novel study on hybrid model of radiative Cu/Fe_3O_4/water nanofluid over a cone with PHF/PWT, The European Physical Journal Special Topics 230 (2021) 1257–1271. https://doi.org/10.1140/epjs/s11734-021-00042-y.

[34] R. Naveen Kumar, R. Gowda, B. Gireesha, B. Prasannakumara, Non-Newtonian hybrid nanofluid flow over vertically upward/downward moving rotating disk in a darcy–forchheimer porous medium, The European Physical Journal Special Topics 230 (2021) 1227–1237. https://doi.org/10.1140/epjs/s11734-021-00054-8.

[35] A. John Christopher, N. Magesh, R. J. Punith Gowda, R. Naveen Kumar, R. S. Varun Kumar, Hybrid nanofluid flow over a stretched cylinder with the impact of homogeneous–heterogeneous reactions and cattaneo–christov heat flux: Series solution and numerical simulation, Heat Transfer 50 (2021) 3800–3821. https://doi.org/10.1002/htj.22052.

[36] P.-Y. Xiong, M. I. Khan, R. P. Gowda, R. N. Kumar, B. Prasannakumara, Y.-M. Chu, Comparative analysis of (zinc ferrite, nickel zinc ferrite) hybrid nanofluids slip flow with entropy generation, Modern Physics Letters B 35 (2021) 2150342. https://doi.org/10.1142/S0217984921503425.

[37] H. Hanif, I. Khan, S. Shafie, A novel study on time-dependent viscosity model of magneto-hybrid nanofluid flow over a permeable cone: Applications in material engineering, The European Physical Journal Plus 135 (2020) 730. https://doi.org/10.1140/epjp/s13360-020-00724-x.

[38] J. Zhao, Axisymmetric convection flow of fractional Maxwell fluid past a vertical cylinder with velocity slip and temperature jump, Chinese Journal of Physics 67 (2020) 501–511. https://doi.org/10.1016/j.cjph.2020.08.009.

[39] M. A. Ezzat, Theory of fractional order in generalized thermoelectric MHD, Applied Mathematical Modelling 35 (2011) 4965–4978. https://doi.org/10.1016/j.apm.2011.04.004.

[40] M. A. Ezzat, Thermoelectric MHD non-Newtonian fluid with fractional derivative heat transfer, Physica B: Condensed Matter 405 (2010) 4188–4194. https://doi.org/10.1016/j.physb.2010.07.009.

Maxwell

ORIGINALITY REPORT

18%	12%	14%	6%
SIMILARITY INDEX	INTERNET SOURCES	PUBLICATIONS	STUDENT PAPERS

PRIMARY SOURCES

1	archive.org Internet Source	1%
2	link.springer.com Internet Source	1%
3	www.archive.org Internet Source	1%
4	Submitted to University of Edinburgh Student Paper	1%
5	Hanifa Hanif. "A finite difference method to analyze heat and mass transfer in kerosene based y-oxide nanofluid for cooling applications", Physica Scripta, 2021 Publication	1%
6	iopscience.iop.org Internet Source	1%
7	Hanifa Hanif. "Cattaneo–Friedrich and Crank–Nicolson analysis of upper-convected Maxwell fluid along a vertical plate", Chaos, Solitons & Fractals, 2021 Publication	1%
8	www.hrvatska21.hr Internet Source	1%

9	Magdy A. Ezzat, Ahmed S. El Karamany. "Fractional order heat conduction law in magneto-thermoelasticity involving two temperatures", Zeitschrift für angewandte Mathematik und Physik, 2011 Publication	1 %
10	apps.dtic.mil Internet Source	<1 %
11	www.akademiabaru.com Internet Source	<1 %
12	bitsavers.trailing-edge.com Internet Source	<1 %
13	Submitted to Indian School of Mines Student Paper	<1 %
14	juen.repo.nii.ac.jp Internet Source	<1 %
15	Hanifa Hanif, Sharidan Shafie. "Interaction of multi-walled carbon nanotubes in mineral oil based Maxwell nanofluid", Scientific Reports, 2022 Publication	<1 %
16	Zafar Said, Sahil Arora, Evangelos Bellos. "A review on performance and environmental effects of conventional and nanofluid-based thermal photovoltaics", Renewable and Sustainable Energy Reviews, 2018 Publication	<1 %
	www.hindawi.com	

17	Internet Source	<1 %
18	R. Naveen Kumar, A.M. Jyothi, Hesham Alhumade, R.J. Punith Gowda et al. "Impact of magnetic dipole on thermophoretic particle deposition in the flow of Maxwell fluid over a stretching sheet", Journal of Molecular Liquids, 2021 Publication	<1 %
19	academic-accelerator.com Internet Source	<1 %
20	semspub.epa.gov Internet Source	<1 %
21	Jamil, M.. "Translational flows of an Oldroyd-B fluid with fractional derivatives", Computers and Mathematics with Applications, 201108 Publication	<1 %
22	K. K. Kalkal, S. Deswal. "Analysis of Vibrations in Fractional Order Magneto-Thermo-Viscoelasticity with Diffusion", Journal of Mechanics, 2014 Publication	<1 %
23	Anuj Kumar Sharma, Arun Kumar Tiwari, Amit Rai Dixit. "Progress of Nanofluid Application in Machining: A Review", Materials and Manufacturing Processes, 2014 Publication	<1 %

24	Submitted to University of Florida Student Paper	<1 %
25	Submitted to South Asian University Student Paper	<1 %
26	hal.archives-ouvertes.fr Internet Source	<1 %
27	www.researchgate.net Internet Source	<1 %
28	Wasim Jamshed, Mohamed R. Eid, Nor Ain Azeany Mohd Nasir, Kottakkaran Sooppy Nisar et al. "Thermal examination of renewable solar energy in parabolic trough solar collector utilizing Maxwell nanofluid: A noble case study", Case Studies in Thermal Engineering, 2021 Publication	<1 %
29	digitallibrary.amnh.org Internet Source	<1 %
30	www.nature.com Internet Source	<1 %
31	www.newspapers.com Internet Source	<1 %
32	F. Mabood, G. P. Ashwinkumar, N. Sandeep. " Effect of nonlinear radiation on 3D unsteady MHD stagnancy flow of Fe O /graphene–water hybrid nanofluid ",	<1 %

	International Journal of Ambient Energy, 2020 Publication	
33	S. Salman, A.R. Abu Talib, S. Saadon, M.T. Hameed Sultan. "Hybrid nanofluid flow and heat transfer over backward and forward steps: A review", Powder Technology, 2020 Publication	<1 %
34	S.R.R. Reddy, C.S.K. Raju, Sreedhara Rao Gunakala, H. Thameem Basha, Se-Jin Yook. "Bio-magnetic pulsatile CuO−Fe3O4 hybrid nanofluid flow in a vertical irregular channel in a suspension of body acceleration", International Communications in Heat and Mass Transfer, 2022 Publication	<1 %
35	WWW.mdpi.com Internet Source	<1 %
36	docshare01.docshare.tips Internet Source	<1 %
37	hdl.handle.net Internet Source	<1 %
38	penerbit.uthm.edu.my Internet Source	<1 %
39	Jinhu Zhao. "Axisymmetric convection flow of fractional Maxwell fluid past a vertical cylinder with velocity slip and temperature jump", Chinese Journal of Physics, 2020 Publication	<1 %

40	Muhammad Jawad, Anwar Saeed, Arshad Khan, Ishtiaq Ali, Hussam Alrabaiah, Taza Gul, Ebenezer Bonyah, Muhammad Zubair. "Analytical study of MHD mixed convection flow for Maxwell nanofluid with variable thermal conductivity and Soret and Dufour effects", AIP Advances, 2021 Publication	<1 %
41	thermalscience.vinca.rs Internet Source	<1 %
42	www.coursehero.com Internet Source	<1 %
43	www.degruyter.com Internet Source	<1 %
44	Hanifa Hanif, Ilyas Khan, Sharidan Shafie. "A novel study on time-dependent viscosity model of magneto-hybrid nanofluid flow over a permeable cone: applications in material engineering", The European Physical Journal Plus, 2020 Publication	<1 %
45	Hanifa Hanif, Sharidan Shafie. "Impact of Al2O3 in Electrically Conducting Mineral Oil-Based Maxwell Nanofluid: Application to the Petroleum Industry", Fractal and Fractional, 2022 Publication	<1 %
46	Hanifa Hanif. "A computational approach for boundary layer flow and heat transfer of	<1 %

fractional Maxwell fluid", Mathematics and Computers in Simulation, 2022
Publication

47 Magdy A. Ezzat, Alla A. El-Bary, Shereen M. Ezzat. "Stokes' first problem for a thermoelectric Newtonian fluid", Meccanica, 2012 <1 %
Publication

48 Sidik, Nor Azwadi Che, Isa Muhammad Adamu, Muhammad Mahmud Jamil, G.H.R. Kefayati, Rizalman Mamat, and G. Najafi. "Recent progress on hybrid nanofluids in heat transfer applications: A comprehensive review", International Communications in Heat and Mass Transfer, 2016. <1 %
Publication

49 V. Puneeth, Rajeev Anandika, S. Manjunatha, Muhammad Ijaz Khan, M. Imran Khan, Ali Althobaiti, Ahmed M Galal. " Implementation of Modified Buongiorno's Model for the Investigation of Chemically Reacting Ternary Nanofluid Jet flow in the Presence of Bio-Active Mixers ", Chemical Physics Letters, 2021 <1 %
Publication

50 Wasim Jamshed. "Numerical investigation of MHD impact on Maxwell nanofluid", International Communications in Heat and Mass Transfer, 2021 <1 %
Publication

51	Xinwei Wang, Xianfan Xu, Stephen U. S. Choi. "Thermal Conductivity of Nanoparticle - Fluid Mixture", Journal of Thermophysics and Heat Transfer, 1999 Publication	<1 %
52	academic.oup.com Internet Source	<1 %
53	doczz.net Internet Source	<1 %
54	dokumen.pub Internet Source	<1 %
55	mdpi-res.com Internet Source	<1 %
56	repositori.uji.es Internet Source	<1 %
57	www.aimspress.com Internet Source	<1 %
58	www.ffpri.affrc.go.jp Internet Source	<1 %
59	www.mdpi.com Internet Source	<1 %
60	www.research.manchester.ac.uk Internet Source	<1 %
61	Luca Deseri, Massiliano Zingales, Pietro Pollaci. "The state of fractional hereditary materials (FHM)", Discrete & Continuous Dynamical Systems - B, 2014	<1 %

Publication

62 Shengting Chen, Liancun Zheng, Bingyu Shen, Xuehui Chen. "Time–space dependent fractional boundary layer flow of Maxwell fluid over an unsteady stretching surface", Theoretical and Applied Mechanics Letters, 2015 <1 %
Publication

63 Syed Asif Ali Shah, Aziz Ullah Awan. "Significance of magnetized Darcy-Forchheimer stratified rotating Williamson hybrid nanofluid flow: A case of 3D sheet", International Communications in Heat and Mass Transfer, 2022 <1 %
Publication

64 Wasim Jamshed, Suriya Uma Devi, Kottakkaran Sooppy Nisar. "Single phase based study of Ag-Cu/EO Williamson hybrid nanofluid flow over a stretching surface with shape factor", Physica Scripta, 2021 <1 %
Publication

65 HongGuang Sun, Yong Zhang, Dumitru Baleanu, Wen Chen, YangQuan Chen. "A new collection of real world applications of fractional calculus in science and engineering", Communications in Nonlinear Science and Numerical Simulation, 2018 <1 %
Publication

Exclude quotes	Off	Exclude matches	Off
Exclude bibliography	On		